

86 GHz Global VLBI Progress Report

S. DOELEMEN¹, A. E. E. ROGERS¹, L. BAÄTH², C. SCHALINSKI³, T. KRICHBAUM⁴,
M. INOUE⁵, A. ZENSUS⁶, S. PADIN⁷, J. CARLSTROM⁷, D. GRAHAM⁴,
C. PREDMORE⁸, J. MORAN⁹, D. BACKER¹⁰, M. WRIGHT¹⁰, N. WHYBORN¹¹,
L. NYMAN¹¹, K. STANDKE⁴, M. LERNER² and S. KAMENO⁵

¹*MIT Haystack Observatory, Westford, MA., U.S.A.*

²*Onsala Space Observatory, Onsala, Sweden*

³*Institut de Radio Astronomie Millimetrique, Grenoble, France*

⁴*Max Planck Institut für Radioastronomie, Bonn, Germany*

⁵*Nobeyama radio Observatory/NAO, Minamimaki, Nagano 384-13, Japan*

⁶*National Radio Astronomy Observatory, Socorro, NM., U.S.A.*

⁷*Owens Valley Radio Observatory, CA., U.S.A.*

⁸*Five College Radio Astronomy Observatory, Amherst, MA., U.S.A.*

⁹*Smithsonian Astrophysical Observatory, Cambridge, MA., U.S.A.*

¹⁰*Radio Astronomy Laboratory, Berkeley, CA., U.S.A.*

¹¹*European Southern Observatory, Santiago, Chile*

Abstract. In April 1993 two 3 mm VLBI campaigns were carried out. One was designed specifically to test the performance of the largest and most sensitive antennae (see elsewhere in these proceedings). The other, described here, utilized the entire 3 mm Global Network of 9 telescopes with a goal of generating high resolution images of bright quasars and AGN. The highest resolution on single baseline detections reached 90 μ s on baselines from Europe to the Western US. The lowest total flux density of a detected source was 1.9 Jy (OJ287).

1. Introduction

3 mm-VLBI experiments have been organized since the early 1980's in an effort to overcome the fundamental limit of angular resolution in radio astronomy. The move to higher frequency also decreases the effects of interstellar scattering and increases the optical depth to which self-absorbed sources can be observed. The ability of the Global VLBI network to operate at 3 mm depends on telescope system temperature, efficiency and recording bandwidth all of which have improved in the last few years. In particular, the Haystack, Effelsberg and Pico Veleta telescopes have just recently joined the network to make its 3 mm VLBI capability much more powerful. While space-VLBI is quite important and can probe higher brightness temperatures, ground based mm-VLBI will remain the highest resolution "instrument" to observe compact sources in the foreseeable future.

2. Network/Observations

An overview of the entire mm network is shown in Table 1.

The inclusion of Haystack, which has recently been resurfaced, Effelsberg, and Pico Veleta greatly increase the sensitivity of the network. Poor weather at Bonn limited detections on Effelsberg baselines, but the intercontinental Haystack-Pico Veleta baseline recorded fringe SNR's of up to 200. Between Haystack and Kitt Peak, SNR's of 100 were recorded on the strongest sources. Use of these large telescopes, in addition to promising high sensitivity imaging, also allows us to search for candidate 3 mm sources using snapshot observations. The SEST telescope in La Silla, Chile was included with N-S resolution in mind. But, despite successful detection of 8 GHz test fringes between SEST and Onsala, no single-baseline 86 GHz fringes have been found to SEST. Nobeyama, OVRO, and Quabbin all experienced some form of LO contamination. In some cases, this can be dealt with during processing as outlined in the example below. Table 2 shows the expected detection thresholds for all baselines.

Table 1. Antennae characteristics.

Station	Symbol	Diameter(m)	Efficiency	T_{sys}
Haystack	H	37	0.15	200
Bonn	B	inner 60	0.13	400
Pico Veleta	P	30	0.55	300
SEST	S	15	0.5	300
Onsala	ON	20	0.48	250
Quabbin	Q	14	0.5	400
KittPeak	K	12	0.55	200
OVRO	OV	3x10	0.55	300
Nobeyama	N	45	0.4	400

Table 2. Detection sensitivities (mJy) - Each element in the detection matrix above assumes an SNR of 3 in a 10 second coherence time with a 56 MHz recording bandwidth.

	H	B	P	S	ON	Q	K	OV	N
H	482								
B	391	317							
P	380	308	300						
S	797	647	629	1333					
ON	557	452	439	922	644				
Q	986	800	778	1633	1141	2020			
K	776	629	612	1284	897	1590	1250		
OV	671	544	529	1104	775	1373	1080	934	
N	485	393	382	803	561	994	782	675	488

All observations were recorded using the Mark III in B-mode (56 MHz) which is compatible with VLBA recorders and which also reduced tape requirements. Data for this portion of the experiment was correlated on Haystack's Mark III correlator and further reduction is underway.

3. Coherence

At 3 mm wavelengths, an important concern is the loss of interferometer coherence due to weather or phase noise in the LO chain. Typical coherence times during good weather are ~ 30 seconds but can be quite variable. The Haystack-Kitt Peak baseline, for example, demonstrated excellent phase stability: a 5% loss in amplitude in 60 seconds. At the other extreme, a faulty H-maser buffer at Quabbin limited coherence times for Haystack-Quabbin to ~ 3 seconds. In the last case, it is still possible to extract meaningful closure phase information if the SNR is sufficient

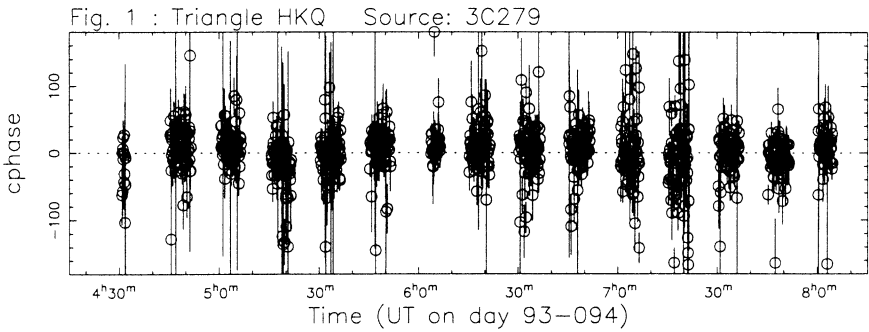


Fig. 1. Closure phase on the Haystack-Kitt Peak-Quabbin triangle segmented to 5 seconds.

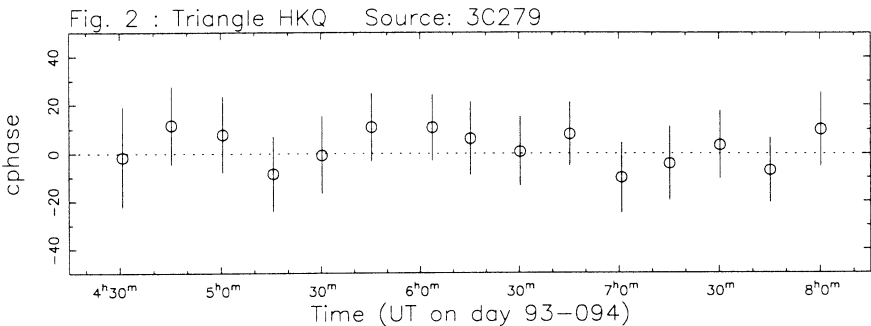


Fig. 2. Closure phase on the same triangle with all segments in a scan vector averaged. Note the change in scale from Fig. 1.

to detect fringes on at least two of three baselines in a triangle. To do this, we first segment the data into finer and finer time slices and plot the vector average of closure phase weighted by the single baseline amplitudes (see ROGERS *et al.*, 1984):

$$\sum_i (Z_{Kk})_i (Z_{kq})_i (Z_{qK})_i \exp\left\{j\left((\phi_{Kk})_i + (\phi_{kq})_i + (\phi_{qK})_i\right)\right\}. \quad (1)$$

Here, Z 's and ϕ 's represent the amplitudes and phases of the i 'th segment. As the coherence time is reached, structure in the plot remains constant even with further reduction of the segment time. Figures 1 and 2 show an example of segmented closure phase for the HKQ triangle and the same plot after a weighted average.

4. Imaging Strategies

With the data now correlated, it is possible to extract more detections by forcing closure on triangles of baselines. If two baselines yield detections then the fringe search windows on the third (undetected) baseline can be narrowed and the search carried out again; this reduces the SNR required for fringe detection. An antenna based algorithm of this sort is given in ALEF and PORCAS (1986). When all possible detections are extracted, the averaging process described above reduces the effect of incoherence in determining closure phase. Ultimately, after pre-image processing, the sources able to be imaged with traditional self calibration techniques will be small. 3C279 and 3C273 are the only sources for which long (u, v) tracks were covered. Most other sources including 2145+067, 0528+134, 3C345, 3C454.3, 3C111, and 3C84 will require model fitting. The remaining detections—OJ287, 1055+018, 0748+126, 1334-127, BL Lac—were essentially snapshots and can be used to estimate compactness.

5. Conclusions

While much processing remains to be done on these observations, it is evident that high angular resolution ($90 \mu\text{as}$) and low detection levels (1.9 Jy) were achieved. These results and the good phase stability on many baselines are encouraging despite the technical and logistical challenges of operating a large network at this frequency.

REFERENCES

- ROGERS, A. E. E., MOFFET, A. T., BACKER, D. C. and MORAN, J. M. (1984): Coherence limits in VLBI observations at 3-millimeter wavelength. *Radio Science*, **19**, 1552–1560.
 ALEF, W. and PORCAS, R. W. (1986): VLBI fringe-fitting with antenna-based residuals. *Astron. Astrophys.*, **168**, 365–368.